



Cite this: *Environ. Sci.: Processes Impacts*, 2025, 27, 2410

Updated global warming potentials of inhaled halogenated anesthetics, isoflurane and sevoflurane from new temperature dependent OH-kinetics†

Sara Espinosa,^{ab} Francisco Martínez,^b María Antiñolo,^b Ole J. Nielsen^b and Elena Jiménez^{ab}

Despite the use of scavenging systems in anesthesia machines, inhaled halogenated anesthetic gases (HAGs), such as isoflurane ($\text{CF}_3\text{CHClOCHF}_2$) and sevoflurane ($(\text{CF}_3)_2\text{CHOCH}_2\text{F}$), are still emitted directly into the atmosphere. In 2014, their atmospheric concentrations were 0.097 ppt (isoflurane) and 0.13 pptv (sevoflurane). As halogenated species, their impact on global warming has to be known. Notably, the global warming potential at a time horizon of 100 years ($\text{GWP}_{100 \text{ years}}$) for sevoflurane differs between IPCC and WMO sources, creating regulatory uncertainty. For that reason, in this work $\text{GWP}_{100 \text{ years}}$ for isoflurane and sevoflurane was reevaluated from the atmospheric chemical lifetimes, $\tau_{\text{HAG}}^{\text{OH}}$, derived from the kinetic study of the gas-phase reactions of hydroxyl (OH) radicals with the HAGs and the radiative efficiencies (REs) derived from the (IR) absorption cross sections in the atmospheric window ($1500\text{--}500 \text{ cm}^{-1}$). The temperature dependence of the OH-rate coefficients ($k_1(T)$ for isoflurane and $k_2(T)$ for sevoflurane) between 263 and 353 K was determined at 100 Torr by using the pulsed laser photolysis/laser-induced fluorescence technique. The obtained Arrhenius expressions are $k_1(T) = (1.1 \pm 0.5) \times 10^{-13} \exp\{-(1234 \pm 144)/T\}$ and $k_2(T) = (1.6 \pm 0.7) \times 10^{-12} \exp\{-(1065 \pm 138)/T\} \text{ cm}^3 \text{ molecule}^{-1} \text{ s}^{-1}$. At 272 K, a $\tau_{\text{HAG}}^{\text{OH}}$ of 3.0 years for isoflurane and 1.2 years for sevoflurane were estimated relative to CH_3CCl_3 from k_1 and k_2 . Moreover, the ultraviolet (UV) absorption cross sections were determined between 190 and 400 nm at 298 K, and the absorption was found to be negligible above 290 nm, indicating minimal photolysis by sunlight. In contrast, the IR absorption in the atmospheric window is significant and the IR absorption cross sections ($4000\text{--}500 \text{ cm}^{-1}$) were determined by Fourier Transform infrared spectroscopy. The lifetime-corrected radiative efficiencies (REs) were 0.44 and 0.30 $\text{W m}^{-2} \text{ ppbv}^{-1}$ for isoflurane and sevoflurane, respectively. From lifetime-corrected REs and $\tau_{\text{HAG}}^{\text{OH}}$, $\text{GWP}_{100 \text{ years}}$ was estimated to be 508 for isoflurane (5% lower than IPCC/WMO values) and 125 for sevoflurane (36% lower than IPCC and 11% lower than WMO). These findings confirm isoflurane to be a high-GWP gas (above 150) according to the EU 2024 regulation, while sevoflurane does not meet the high-GWP threshold. A reassessment of the IPCC and WMO values is recommended.

Received 24th January 2025

Accepted 4th June 2025

DOI: 10.1039/d5em00061k

rsc.li/espi

^aUniversidad de Castilla-La Mancha (UCLM), Facultad de Ciencias y Tecnologías Químicas, Departamento de Química Física, Avda. Camilo José Cela, 1B, 13071 Ciudad Real, Spain. E-mail: Elena.Jimenez@uclm.es

^bInstituto de Investigación en Combustión y Contaminación Atmosférica (ICCA), UCLM, Camino de Moledores, s/n, 13071 Ciudad Real, Spain

^cCopenhagen Centre for Atmospheric Research, Department of Chemistry, University of Copenhagen, Copenhagen, Denmark

† Electronic supplementary information (ESI) available: Tables S1 and S2 present the experimental conditions and individual rate coefficients for the $\text{OH} + \text{CF}_3\text{CHClOCHF}_2$ (Isoflurane) and $\text{OH} + (\text{CF}_3)_2\text{CHOCH}_2\text{F}$ (Sevoflurane) reactions. Tables S3 and S4 show a comparison with literature data of the IR absorption peaks and integrated absorption cross sections for the investigated HAGs. Table S5 presents a summary of the atmospheric lifetimes of HAGs due to the gas-phase reaction with OH radicals estimated in this

work and in the literature. Fig. S1 shows a schematic of the introduction of gases in a jacketed reaction cell. Fig. S2 shows examples of the calibration plots of the mass flow controllers used for diluted mixtures of isoflurane and sevoflurane. Fig. S3 presents some examples of the comparison of HAG concentration from flow measurements and from IR spectroscopy. Fig. S4 presents several examples of the temporal evolution of $\ln I_{\text{LIF}}$ in the presence of a similar concentration of the halogenated anesthetics at several temperatures. Fig. S5 shows some examples of the bimolecular plots at 253 K, 298 K, and 423 K at a similar $[\text{HAG}]$ ($\sim 1.2 \times 10^{16} \text{ molecules cm}^{-3}$) for (A) isoflurane and (B) sevoflurane. Fig. S6 and S7 present examples of Beer-Lambert's plots at several IR wavenumbers for both HAGs and several UV wavelengths for isoflurane. In Fig. S8 the UV absorption spectrum for isoflurane and the spectral actinic flux are overlapped. See DOI: <https://doi.org/10.1039/d5em00061k>



Environmental significance

The healthcare sector must reduce its carbon footprint, including emissions from anesthetic gases like isoflurane and sevoflurane, which are released directly into the atmosphere (~ 0.1 ppt). To prioritize mitigation efforts, accurate global warming potentials of these gases are essential. This study evaluates their primary degradation pathway in the troposphere—reaction with OH radicals (estimation of atmospheric lifetimes)—and their radiative efficiencies through the experimental IR absorption cross sections in the atmospheric window. Although photolysis in the troposphere is unlikely, UV absorption cross sections (190–400 nm) were analyzed to address discrepancies in existing data. These findings are crucial for understanding the environmental impact of these anesthetics and guiding strategies to minimize their contribution to global warming over 100 years.

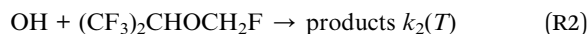
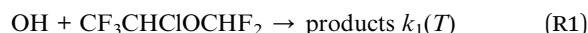
1. Introduction

Inhaled anesthetics are used worldwide for clinical interventions, either in humans or animals, and most of them are eliminated by exhalation (>70%) without being metabolized (0.2–5%).¹ In the 1980s, halogenated anesthetic gases (HAGs) replaced nitrous oxide (N_2O), used since the XIX century as an anesthetic gas. Its declining role in general anesthesia is driven by a mix of environmental concerns, clinical risks, and the availability of better anesthetics. As the world population keeps growing and modern anesthesia becomes available in more regions of the world, the global use and emissions of HAGs are expected to grow.² In 2022, more than 3.3 million surgical interventions were performed in Spain according to data released by the Spanish National Health System in 2023.³ Despite the introduction of scavenging systems (based on silica zeolites, for example) in anesthesia machines, most HAGs are still released directly into the atmosphere.² For example, isoflurane ($\text{CF}_3\text{CHClOCHF}_2$, HCFE-235da2) and sevoflurane ($(\text{CF}_3)_2\text{CHOCH}_2\text{F}$, HFE-347mmz1) (Fig. 1) presented atmospheric abundances in 2014 of around 0.097 and 0.13 ppt, respectively.⁴ In 2019, inhaled anesthetics were responsible for around 5% of the healthcare-related climate footprint in England.^{4,5}

Even though the use of fluorinated gases (F-gases) in the European Union (EU) declined by 37% in metric tons and by 47% in terms of tons of CO_2 equivalent from 2015 to 2019, the EU commission presented a new regulation on emission prevention measures of F-gases, including isoflurane in 2024.⁶ This EU regulation defines a high global warming potential (GWP) relative to CO_2 to values above 150. For isoflurane, the International Panel on Climate Change (IPCC)⁷ and the World Meteorological Organization (WMO)⁸ recommend a GWP at a horizon time of 100 years ($\text{GWP}_{100\text{years}}$) of 539 and 536, respectively. So, according to the EU regulation isoflurane is

a potent greenhouse gas with higher $\text{GWP}_{100\text{ years}}$ than N_2O ($\text{GWP}_{100\text{ years}} = 273$).⁷ However, N_2O remains a major contributor to climate change due to its widespread use.⁹ In contrast, the recommended $\text{GWP}_{100\text{ years}}$ for sevoflurane varies depending on the source ($\text{GWP}_{100\text{ years}} = 195$ ⁷ and $\text{GWP}_{100\text{ years}} = 140$ ⁸) and it falls under the scope of the EU regulation or not.

For long-lived species, the atmospheric lifetime (τ) is often estimated from the OH radical (τ_{OH}) reactivity relative to that of methyl chloroform (CH_3CCl_3) at a mean tropospheric temperature of 272 K. As the main atmospheric fate of these HAGs is the reaction with hydroxyl (OH) radicals, $\tau_{\text{HAG}}^{\text{OH}}$ of isoflurane and sevoflurane directly impacts the GWP calculation. Sulbaek Andersen *et al.*¹⁰ first used an estimation of the rate coefficients for the OH-reactions for isoflurane (reaction (R1)) and sevoflurane (reaction (R2)) at 272 K to estimate $\tau_{\text{HAG}}^{\text{OH}}$. These authors derived $k_1(273\text{ K})$ and $k_2(273\text{ K})$ from calculated Arrhenius parameters using the method described by DeMore.¹¹



Using the temperature dependencies of $k_1(T)$ in the range of 250–430 K¹² and $k_2(T)$ in the range of 241–298 K,¹³ $\text{GWP}_{100\text{ years}}$ was recalculated by Sulbaek Andersen *et al.*¹³ For isoflurane, no change in $\text{GWP}_{100\text{ years}}$ ($=510$) was reported. However, these authors recommended in 2023¹⁴ a $\text{GWP}_{100\text{ years}}$ of 539 as reported by the IPCC (2023).⁷ For sevoflurane, the recalculated $\text{GWP}_{100\text{ years}}$ changed from 210 to 130 ($\sim 40\%$ reduction).¹³ Nevertheless, a new correction of $\text{GWP}_{100\text{ years}}$ was reported by Sulbaek Andersen *et al.*¹⁵ based on the current JPL¹⁶ recommendation and the updated GWP calculation method,¹⁷ changing from 130 to 144 ($\sim 10\%$ increase). The variability of $\text{GWP}_{100\text{ years}}$ in these studies is mainly due to the different methods used for calculating REs and $\tau_{\text{HAG}}^{\text{OH}}$, estimated from the rate coefficients. For isoflurane and sevoflurane, lifetime-corrected REs do not differ greatly. Therefore, the difference in reported GWPs may be due to $\tau_{\text{HAG}}^{\text{OH}}$ estimated from the rate coefficients, highlighting the importance of measuring them. Additionally, for sevoflurane, it is crucial to determine whether it falls within the scope of the EU regulation,⁶ which imposes some limitations on F-gases with a $\text{GWP}_{100\text{ years}} > 150$.

In the literature, several kinetic studies on reactions (R1) and (R2) have been found, especially at around room temperature (293–300 K). Particularly, the kinetics of reaction (R1) has been widely investigated by absolute^{13,18–20} and relative kinetic techniques,^{12,19,21,22} determining $k_1(298\text{ K})$ at low pressures (2.0–6.3 Torr) using the discharge flow-resonance fluorescence (DF-RF)

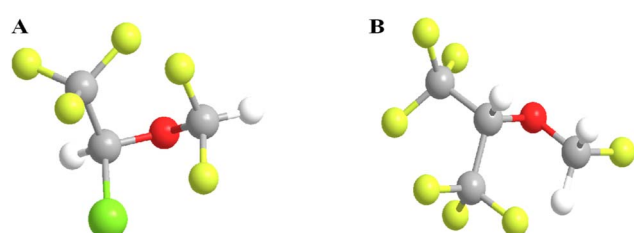


Fig. 1 Chemical structures of (A) isoflurane ($\text{CF}_3\text{CHClOCHF}_2$, HCFE-235da2) and (B) sevoflurane ($(\text{CF}_3)_2\text{CHOCH}_2\text{F}$, HFE-347mmz1).



technique. At higher total pressures (50 mbar \equiv 37.5 Torr), Langbein *et al.*²⁰ used the laser long-path absorption (LLPA) technique to monitor OH radicals and, more recently, Sulbaek Andersen *et al.*¹³ employed the pulsed laser photolysis-laser induced fluorescence (PLP-LIF) technique to determine k_1 (298 K) at 111 Torr. At atmospheric pressure (760 Torr), Nolan *et al.*²¹ determined k_1 (298 K) using a relative method using gas chromatograph coupled to a flame ionization detector (GC/FID) and Fourier Transform Infrared (FTIR) spectroscopy as detection techniques of the anesthetics and the reference compound. Between 2.0 and 760 Torr, no pressure dependence of k_1 (298 K) was observed.

Regarding the temperature dependence of $k_1(T)$, there are two absolute kinetic studies in the literature. Tokuhashi *et al.*¹² combined DF and photolysis methods coupled to RF detection of OH radicals to determine $k_1(T)$ between 250 and 430 K in the 5–60 Torr interval, whereas Beach *et al.*²² measured $k_1(T)$ above 293 K up to 393 K. The observed temperature dependencies of $k_1(T)$ by these two groups are not in agreement. Activation energies (E_a) and pre-exponential factors (A) obtained by Beach *et al.*²² ($E_a = 7.8 \pm 0.8$ kJ mol⁻¹ and $A = (4.5 \pm 1.3) \times 10^{-12}$ cm³ molecule⁻¹ s⁻¹) and Tokuhashi *et al.*¹² ($E_a = 10.6 \pm 0.8$ kJ mol⁻¹ and $A = (1.12 \pm 0.18) \times 10^{-12}$ cm³ molecule⁻¹ s⁻¹) differ by more than 25% and 75%, respectively. The Arrhenius parameters E_a and A are essential to accurately derive the rate coefficient at 272 K, an appropriate temperature to estimate the atmospheric lifetime of long-lived species, such as the HAGs. Therefore, an additional kinetic study on the temperature dependence of $k_1(T)$ is needed.

The rate coefficient for the reaction (R2) has been widely investigated at room temperature, k_2 (298 K), by absolute methods.^{13,18–20} No agreement is found among the results of the four previous kinetic studies for reaction (R2). The reported k_2 (298 K) range from 2.7 to 7.3×10^{-14} cm³ molecule⁻¹ s⁻¹, so it is needed to perform an additional study to elucidate which $k_2(T)$ is correct. The only comprehensive kinetic study of $k_2(T)$ as a function of temperature was performed by Sulbaek Andersen *et al.*¹³ by PLP-LIF between 298 and 241 K at 111 Torr and at 243 K and 300 Torr. The temperature dependence study of $k_2(T)$ is recommended to be extended to higher temperatures also to gain insight into the kinetic behavior of sevoflurane. For that reason, in this work, we revisited the temperature dependencies of $k_1(T)$ and $k_2(T)$ between 253 and 423 K at 100 Torr of helium using the PLP-LIF technique.

Ultraviolet (UV) photolysis of hydrofluoroethers, like isoflurane and sevoflurane, in the solar actinic region ($\lambda > 290$ nm) is not expected to occur. However, these species strongly absorb in the vacuum UV (VUV) region and the UV spectra of isoflurane and sevoflurane have been reported at 298 K between 115 and 350 nm.^{20,23} Particularly, Langbein *et al.*²⁰ recorded the UV spectra of HAGs in the wavelength range of 200–350 nm, providing the absorption cross sections (in base 10) between 200 and 230 nm. These authors found that isoflurane and sevoflurane do not absorb at wavelengths longer than 215 nm and 200 nm, respectively. More recently, Lange *et al.*²³ recorded the high-resolution (0.1 nm) VUV spectra using synchrotron radiation over the 115–248 nm range, corresponding to photon

energies between 5.0 and 10.8 eV. These authors reported the VUV absorption cross sections in megabarn, 1 Mb $\equiv 10^{-18}$ cm², and they were compiled (in base e) between 115 and 340 nm in the MPI-Mainz UV/vis spectral atlas.²⁴ However, after scaling the reported UV absorption cross sections to the same base (base e) there is a disagreement, especially for sevoflurane, between the studies of Langbein *et al.*²⁰ and Lange *et al.*²³ above 200 nm. Therefore, in this work, the absolute UV absorption cross sections were also determined between 190 and 400 nm at 298 K. Langbein *et al.*²⁰ and Lange *et al.*²³ also calculated the photochemical atmospheric lifetimes of isoflurane and sevoflurane up to 36 km and up to 50 km, respectively, assuming a photolysis quantum yield of 1. These authors concluded that these HAGs were not degraded in the troposphere and stratosphere by photolysis.

As stated above, in addition to the OH-kinetics, the infrared (IR) spectra of isoflurane and sevoflurane are crucial to properly assess the GWP calculation of these HAGs. Currently, there is no agreement between the studies of Brown *et al.*^{18,19} and Sulbaek Andersen *et al.*¹⁰ Brown *et al.*¹⁸ recorded the IR spectra of isoflurane and sevoflurane between 1200 and 600 cm⁻¹ at a resolution of 2.40 cm⁻¹. The IR absorption cross sections are systematically lower than those reported by Sulbaek Andersen *et al.*¹⁰ who reported them between 2000 and 650 cm⁻¹ at a much higher resolution, 0.25 cm⁻¹. Therefore, the present work may elucidate this discrepancy by determining the absolute IR absorption cross sections of these HAGs between 500 and 4000 cm⁻¹ at a resolution of 0.5 cm⁻¹. In addition, integrated IR absorption cross sections in the range of 800–1200 cm⁻¹ and 650–1500 cm⁻¹ are reported here for both HAGs for comparing with those from Sulbaek Andersen *et al.*¹⁰ and Brown *et al.*¹⁹

2. Experimental section

2.1. Absolute gas-phase kinetics of OH-reactions

The experimental system used in this work to determine the second-order rate coefficient, $k_i(T)$ ($i = 1$ or 2), was described elsewhere.^{25–27} Briefly, the OH radicals were generated *in situ* in a jacketed Pyrex® reactor ($V \sim 200$ cm³) by PLP at 248 nm of a OH-precursor, either hydrogen peroxide (H₂O₂) or nitric acid (HNO₃). UV radiation was provided by using a KrF excimer laser (Coherent, mod. Excistar 200). The OH radicals were excited at 282 nm by the second harmonic of a rhodamine-6G dye laser (LiopTech, mod. LiopStar) pumped by the second harmonic of an Nd-YAG laser (InnoLas, mod. SpitLight 1200). Laser induced fluorescence from excited OH radicals was collected at around 310 nm as a function of the reaction time.

All gases were introduced into the reactor by calibrated mass flow controllers (MFCs). As the investigated reactions are very slow, large mixing ratios of the HAG in helium ($f = p_{\text{HAG}}/750$ Torr, where $p_{\text{HAG}} = 70$ –80 Torr) were needed ($f = (9.2 \times 10^{-2} - 1.2 \times 10^{-1})$, as shown in Tables S1 and S2 of the ESI.† As the HAG/He mixture had no similar properties (density, thermal conductivity and heat capacity) compared to the gases used in the factory calibration (He among others), the MFC had to be calibrated for each HAG/He mixture used in the kinetic



experiments. Examples of the calibration of the mass flow rate of HAG/He mixtures are shown in Fig. S2.† Tables S1 and S2† also summarize the mass flow rates employed in the experiments at the investigated temperature (253–423 K) for HAG/He ($F_{\text{HAG/He}}$), OH-precursor/He (F_{Prec}) and He (F_{He}). By changing F_{R} and the total flow rate, [HAG] in the reactor was varied ([isoflurane] = $(0.18 - 6.91) \times 10^{16}$ molecules cm^{-3} and [sevoflurane] = $(0.17 - 6.88) \times 10^{16}$ molecules cm^{-3}). In addition to the mass flow controller calibration, the mixing ratio of isoflurane and sevoflurane was checked off-line by recording IR spectra as a function of the HAG mass flow rate and using the IR absorption cross sections determined in this work (more details in the ESI†).

Under pseudo-first order conditions (*i.e.* HAG in large excess with respect to OH radicals), the LIF signal (I_{LIF}) follows a single exponential function. Some examples of the linearized temporal evolution plots of I_{LIF} at several temperatures are shown in Fig. S4.† For a given HAG concentration, [HAG], and temperature, the pseudo-first order coefficient (k') is obtained from the slope of the corresponding linearized I_{LIF} decay. The total pressure was set to 100 Torr of helium. Under these conditions, there is a linear relationship between k' and [HAG], as shown in eqn (E1).

$$k' = k_i(T)[\text{HAG}] + k'_0 \quad (\text{E1})$$

In the absence of HAGs, the loss of OH is due to the reaction with the OH-precursor and diffusion out of the detection zone (k'_0). The individual second-order rate coefficients, $k_i(T)$ were determined from $k' - k'_0$ vs. [HAG] plots. Fig. S5† shows examples of plots of eqn (E1) for the OH-reaction at room temperature and at the minimum and maximum temperatures investigated in this work, 253 K and 423 K and at a total pressure of 100 Torr.

The presence of reactive impurities may affect the measured rate coefficient. In the present work, the purity of the HAG samples was investigated by GC (Shimadzu, GC-2010 Plus) coupled to a time-of-flight mass spectrometer (ToF-MS, Jeol, AccuTOF GCv) for peak identification. The GC used is equipped with an Equity-1701 column (30 m × 0.32 mm I.D., 1 μm) and the gaseous sample (1 μL) was injected into the GC with a temperature ramp set as 35 °C for 2 min, then 5 °C min^{-1} to 100 °C, 10 °C min^{-1} to 200 °C, and 25 °C min^{-1} to 250 °C. In both HAG samples, the chromatogram did not show other peaks. A purity of >99.8% for both HAGs was estimated from the ratio of the peak intensity and the baseline of the chromatogram.

2.2. IR and UV absorption spectroscopy in the gas-phase

The experimental set-ups have been already described in previous studies.^{27–29} The IR absorption spectra of the HAGs were recorded between 4000 and 500 cm^{-1} using a FTIR spectrometer (Bruker, Tensor 27). The instrumental resolution of the FTIR spectrometer was set to 0.5 cm^{-1} corresponding with a data spacing of around 0.24 cm^{-1} . A single path stainless steel cell ($\ell = 10 \pm 0.2$ cm) was used to measure the absorbance at each wavenumber ($A_{\tilde{\nu}}$) under static conditions. The absorption

cell was filled with pure isoflurane (0.8–2.8 Torr) or sevoflurane (1.4–3.3 Torr) at room temperature, yielding concentration ranges of $(2.46 - 9.20) \times 10^{16}$ and $(0.46 - 1.08) \times 10^{17}$ molecules cm^{-3} , respectively.

The UV absorption spectroscopy system consists of a UV jacketed Pyrex® cell ($\ell = 107.0 \pm 0.2$ cm). The UV spectra of isoflurane and sevoflurane between 190 and 400 nm were recorded under static conditions at room temperature. An instrumental resolution of 3 nm yields a data spacing of 0.5 nm. The experiments were carried out by introducing into the UV cell a certain pressure of the HAG ((5.5–35.0 Torr) of isoflurane and (6.0–46.9 Torr) of sevoflurane), yielding concentration ranges of [isoflurane] = $(0.18 - 1.14) \times 10^{18}$ molecules cm^{-3} and [sevoflurane] = $(0.19 - 1.53) \times 10^{18}$ molecules cm^{-3} .

From the slope of the Beer–Lambert's plot eqn (E2) at each wavenumber, $\tilde{\nu}$, the IR absorption cross sections (in base e), $\sigma_{\tilde{\nu}}$, were derived.

$$A_{\tilde{\nu}} = \sigma_{\tilde{\nu}} \ell [\text{HAG}] \quad (\text{E2})$$

In Fig. S6† (panels A and C), some examples of $A_{\tilde{\nu}}$ vs. [HAG] plots are shown for selected wavenumbers, all presenting good linearity in the entire concentration range. In addition to the absolute $\sigma_{\tilde{\nu}}$, the integrated IR absorption cross sections, $S_{\text{int}}(\tilde{\nu}_1 - \tilde{\nu}_2)$ given by eqn (E3) were determined in certain wavenumber ranges by applying Beer–Lambert's law, expressed in terms of the integrated absorbance, A_{int} (Fig. S6† – panels B and D).

$$S_{\text{int}}(\tilde{\nu}_1 - \tilde{\nu}_2) = \int_{\tilde{\nu}_1}^{\tilde{\nu}_2} \sigma_{\tilde{\nu}} d_{\tilde{\nu}} \quad (\text{E3})$$

A total of 7–9 IR spectra were used to determine $\sigma_{\tilde{\nu}}$ and $S_{\text{int}}(\tilde{\nu}_1 - \tilde{\nu}_2)$.

In a similar way, the UV absorption cross sections for isoflurane, at a wavelength λ , σ_{λ} (in base e), were determined by applying eqn (E2) in terms of λ , *i.e.* σ_{λ} is obtained from the slope of the A_{λ} vs. [HAG] plot (Fig. S7†). In contrast, no absorption was observed for sevoflurane in the 190–400 nm wavelength range.

2.3. Chemicals

Helium (99.999%, Nippon Gases) and an aqueous solution of HNO_3 (65% w/w, Scharlab) were used as supplied. The aqueous solution of H_2O_2 (>50% v/v, Scharlab) was pre-concentrated as described in Albaladejo *et al.*²⁵ Liquid $\text{CF}_3\text{CHClOCH}_2\text{F}$ (95%, Chemspace) and $(\text{CF}_3)_2\text{CHOCH}_2\text{F}$ (95%, Chemspace) were used after degasification by several freeze–pump–thaw cycles.

3. Results and discussion

3.1. Temperature dependence of $k_1(T)$ and $k_2(T)$

The individual $k_1(298 \text{ K})$ and $k_2(298 \text{ K})$ together with the experimental conditions used in the kinetic study are listed as a function of temperature in Tables S1 and S2.† The rate coefficients at a single temperature provided in Table 1 were determined from the average of the rate coefficients obtained from $k' - k'_0$ vs. [HAG] plots (Fig. S5†). Over the temperature range investigated, the obtained rate coefficients are relatively low. $k_1(T)$ was on the order of 10^{-15} – 10^{-14} $\text{cm}^3 \text{molecule}^{-1} \text{s}^{-1}$



Table 1 Summary of the rate coefficients obtained in this work for the OH-reactions with isoflurane ($k_1(T)$) and sevoflurane ($k_2(T)$) as a function of temperature. Uncertainties are $\pm 2\sigma$ including both statistical and estimated systematic uncertainties

| T/K | $k_1(T)/10^{-14} \text{ cm}^3 \text{ molecule}^{-1} \text{ s}^{-1}$ | $k_2(T)/10^{-14} \text{ cm}^3 \text{ molecule}^{-1} \text{ s}^{-1}$ |
|-----|---|---|
| 253 | 0.80 ± 0.17 | 2.53 ± 0.51 |
| 263 | 1.02 ± 0.22 | 2.76 ± 0.59 |
| 273 | 1.17 ± 0.23 | 2.89 ± 0.68 |
| 283 | 1.39 ± 0.28 | 3.54 ± 0.73 |
| 298 | 1.96 ± 0.41 | 4.25 ± 0.86 |
| 323 | 2.84 ± 0.61 | 5.78 ± 1.33 |
| 353 | 3.49 ± 0.77 | 7.85 ± 1.75 |
| 393 | 4.45 ± 1.18 | 10.1 ± 2.0 |
| 423 | 5.47 ± 1.59 | 13.3 ± 3.1 |

and $k_2(T)$ was about one order of magnitude larger (10^{-14} – 10^{-13} $\text{cm}^3 \text{ molecule}^{-1} \text{ s}^{-1}$). At room temperature, for example, $k_1(298 \text{ K}) = (1.96 \pm 0.41) \times 10^{-14} \text{ cm}^3 \text{ molecule}^{-1} \text{ s}^{-1}$ and $k_2(298 \text{ K}) = (4.25 \pm 0.86) \times 10^{-14} \text{ cm}^3 \text{ molecule}^{-1} \text{ s}^{-1}$. Both $k_1(T)$ and $k_2(T)$ increase with increasing temperature. The difference in $k_1(253 \text{ K})$ with respect to $k_1(423 \text{ K})$ is 86% for isoflurane and 81% for sevoflurane.

A weighted fit of the rate coefficients to the Arrhenius expressions yields eqn (E4) and (E5):

$$k_1(T) = (1.1 \pm 0.5) \times 10^{-13} \exp\{-(1234 \pm 144)/T\} \text{ cm}^3 \text{ molecule}^{-1} \text{ s}^{-1} \quad (\text{E4})$$

$$k_2(T) = (1.6 \pm 0.7) \times 10^{-12} \exp\{-(1065 \pm 138)/T\} \text{ cm}^3 \text{ molecule}^{-1} \text{ s}^{-1} \quad (\text{E5})$$

Uncertainties in the pre-exponential factor A and E_a/R factors correspond to $\pm 2\sigma$ obtained from the fit of the kinetic data to eqn (E1). A positive temperature dependence of $k_i(T)$ was observed for both HAGs between 253 and 423 K, with activation energies (E_a) of $(10.3 \pm 1.2) \text{ kJ mol}^{-1}$ and $(8.9 \pm 1.1) \text{ kJ mol}^{-1}$ for reactions (R1) and (R2), respectively. The Arrhenius expressions given by eqn (E4) and (E5) are depicted in Fig. 2 as thick black lines.

There are two previous studies on the temperature dependence of $k_1(T)$. Tokuhashi *et al.*¹² (eqn (E6), blue line in Fig. 2A) and Beach *et al.*²² (eqn (E7), red line in Fig. 2A) reported the following Arrhenius expressions (uncertainties $\pm 2\sigma$).

$$k_1(T = 250 - 430 \text{ K}) = (1.12 \pm 0.36) \times 10^{-12} \exp\{-(1280 \pm 100)/T\} \text{ cm}^3 \text{ molecule}^{-1} \text{ s}^{-1} \quad (\text{E6})$$

$$k_1(T = 293 - 393 \text{ K}) = (4.5 \pm 1.3) \times 10^{-13} \exp\{-(940 \pm 100)/T\} \text{ cm}^3 \text{ molecule}^{-1} \text{ s}^{-1} \quad (\text{E7})$$

Although Brown *et al.*¹⁹ reported an Arrhenius expression (eqn (E8), purple line in Fig. 2B) for the temperature dependence of $k_2(T)$, it was based on two single temperature measurements at 302 and 423 K.

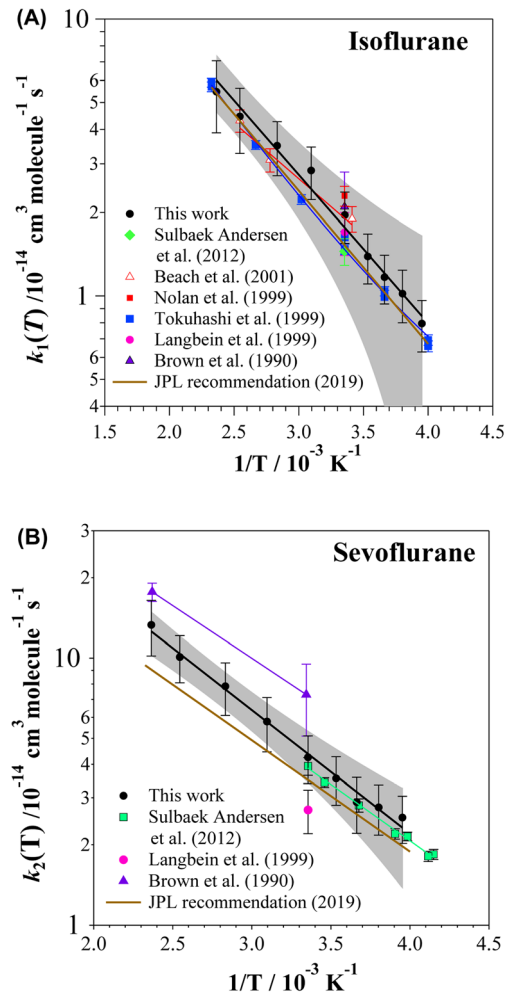


Fig. 2 Arrhenius plots of $k_i(T)$ obtained in this work together with the previously reported kinetic data for (A) isoflurane and (B) sevoflurane. Quoted errors are statistical $\pm 2\sigma$. Shaded zones are the prediction bands at a 95% confidence level.

$$k_2(T = 302, 423 \text{ K}) = 1.53 \times 10^{-12} \exp\{-(900 \pm 500)/T\} \text{ cm}^3 \text{ molecule}^{-1} \text{ s}^{-1} \quad (\text{E8})$$

Therefore, the only comprehensive study on the temperature dependence of $k_2(T)$ was carried out by Sulbaek Andersen *et al.*,¹³ who reported the Arrhenius expression given by eqn (E9) (green line in Fig. 2B, uncertainties in the Arrhenius parameters $\pm 2\sigma$).

$$k_2(T = 241 - 298 \text{ K}) = (9.98 \pm 3.24) \times 10^{-13} \exp\{-(969 \pm 82)/T\} \text{ cm}^3 \text{ molecule}^{-1} \text{ s}^{-1} \quad (\text{E9})$$

Table 2 shows a comparison of the Arrhenius parameters obtained in this work with those from the literature. If uncertainties in reported A and E_a for reactions (R1) and (R2) are considered, the results reported in this work are in agreement with those determined by Beach *et al.*²² and Tokuhashi *et al.*¹² for (R1) and from Brown *et al.*¹⁹ and Sulbaek Andersen *et al.*¹³ for reaction (R2). Current JPL¹⁶ recommendations (brown line in Fig. 2A) for the Arrhenius parameters for reaction (R1) are $A =$



Table 2 Comparison of $k_1(298\text{ K})$ and Arrhenius parameters obtained in this work with those from the literature. Uncertainties are $\pm 2\sigma$ statistically

| Anesthetic | T/K | P/Torr | $k_i(298\text{ K})/10^{-14}\text{ cm}^3\text{ molecule}^{-1}\text{ s}^{-1}$ | $A/10^{-12}\text{ cm}^3\text{ molecule}^{-1}\text{ s}^{-1}$ | $(E_a/R)/\text{K}$ | $E_a/\text{kJ mol}^{-1}$ | Technique ^b | Reference |
|-------------|-------------|---------------|---|---|--------------------|--------------------------|------------------------|--|
| Isoflurane | 253–423 | 100 | 1.96 ± 0.41 | 1.1 ± 0.5 | 1234 ± 144 | 10.3 ± 1.2 | PLP-LIF | This work |
| | 295 \pm 4 | 111 | 1.5 ± 0.2 | 4.5 ± 1.3 | 940 ± 100 | 7.8 ± 0.8 | PLP-LIF | Sulbaek Andersen <i>et al.</i> ¹³ |
| | 293–393 | 2.0–3.4 | 1.9 ± 0.2^a | 1.12 ± 0.36 | 1280 ± 100 | 10.6 ± 1.6 | DF-RF | Beach <i>et al.</i> ²² |
| | 250–430 | 20–40 | 1.48 ± 0.12 | 1.48 ± 0.14 | | | FP-LIF | Tokuhashi <i>et al.</i> ¹² |
| | 20–40 | | 1.48 ± 0.14 | | | | PLP-LIF | Tokuhashi <i>et al.</i> ¹² |
| | 5–6 | | 1.63 ± 0.16 | | | | DF-LIF | Tokuhashi <i>et al.</i> ¹² |
| Sevoflurane | 760 | 2.3 \pm 0.2 | | | | | RR | Nolan <i>et al.</i> ²¹ |
| | 298 | 37.5 | 1.7 ± 0.3 | | | | GC-FID and FTIR | |
| | 298 | 3–6.3 | 2.1 ± 0.7 | | | | PLP-LLPA | Langbein <i>et al.</i> ²⁰ |
| | 253–423 | 100 | 4.25 ± 0.86 | | | | DF-RF | Brown <i>et al.</i> ¹⁹ |
| | 241–298 | 111 | 3.9 ± 0.3 | 0.998 ± 0.324 | 1065 ± 138 | 8.9 ± 1.2 | PLP-LIF | This work |
| | 295 \pm 4 | 700 | 3.5 ± 0.7 | 2.7 ± 0.5 | 969 ± 82 | 8.1 ± 0.7 | PLP-LIF | Sulbaek Andersen <i>et al.</i> ¹³ |
| | 298 | 37.5 | | | | | RR/FTIR | Sulbaek Andersen <i>et al.</i> ²⁰ |
| | 302, 423 | 1.9 | | 1.53 | 900 ± 500 | 7.5 ± 4.2 | PLP-LIPA | Langbein <i>et al.</i> ²⁰ |
| | | | | 7.3 ± 2.2 | | | DF-RF | Brown <i>et al.</i> ¹⁹ |

^a $k_1(293\text{ K})$. ^b PLP-LIF: pulsed laser photolysis-laser induced fluorescence; DF-RF: discharge flow resonance fluorescence; LLPA: laser longpath absorption ionization detection; FTIR: fourier transform infrared spectroscopy; PLP-LIPA: pulsed laser photolysis-laser induced fluorescence; RR: relative rate; GC-FID: gas chromatography-flame

$1.1 \times 10^{-12}\text{ cm}^3\text{ molecule}^{-1}\text{ s}^{-1}$ and $E_a/R = 1275\text{ K}$ in the 250–430 K range (with parameters $f(298\text{ K}) = 1.07$ and $g = 50$ that can be used to calculate an estimated rate constant uncertainty at any given temperature). The recommended value for E_a/R is derived from the fit to the two temperature dependent data sets of Tokuhashi *et al.*¹² For the OH + sevoflurane reaction, the Arrhenius expression recommended by JPL (brown line in Fig. 2B) is based on the absolute rate coefficients from Sulbaek Andersen *et al.*¹³ The recommended Arrhenius parameters were $E_a/R = 960\text{ K}$ and $A = 8.77 \times 10^{-13}\text{ cm}^3\text{ molecule}^{-1}\text{ s}^{-1}$ in the 241–422 K range ($f(298\text{ K}) = 1.15$; $g = 100$).

3.1.1. Comparison of $k_1(298\text{ K})$ and $k_2(298\text{ K})$ with previous studies. Table 2 summarizes a comparison of $k_1(298\text{ K})$ and $k_2(298\text{ K})$ with those previously reported in the literature at different total pressures using kinetic techniques. The reported $k_1(298\text{ K})$ and $k_2(298\text{ K})$ were determined by absolute kinetic methods at total pressures below 111 Torr, except that from Nolan *et al.*²¹ and Sulbaek Andersen *et al.*¹³ who employed relative rate methods at 760 and 700 Torr, respectively.

For isoflurane, no pressure dependence of $k_1(298\text{ K})$ is observed, within the stated uncertainties, independent of the kinetic technique. $k_1(298\text{ K})$ is in reasonable agreement with previously reported $k_1(298\text{ K})$, especially considering that measuring very low rate coefficients, such as k_1 , is absolutely challenging. $k_1(298\text{ K})$ reported in this work is in good agreement, within the error limits, with $k_1(298\text{ K})$ reported by Brown *et al.*,¹⁹ Beach *et al.*,²² and Langbein *et al.*²⁰ $k_1(298\text{ K})$ determined in this work is slightly lower than the relative $k_1(298\text{ K})$ reported by Nolan *et al.*,²¹ whereas it is higher than absolute $k_1(298\text{ K})$ determined by Tokuhashi *et al.*¹² and Sulbaek Andersen *et al.*¹³

For sevoflurane, there is a good agreement between $k_2(298\text{ K})$ determined in this work and that reported by Sulbaek Andersen *et al.*¹³ by PLP-LIF (111 Torr) and RR/FTIR (700 Torr). In contrast, $k_2(298\text{ K})$ determined in this work is much higher than that reported by Langbein *et al.*²⁰ The opposite is observed when compared with Brown *et al.*'s¹⁹ work, and $k_2(298\text{ K})$ reported in this work is lower. This was also observed by Sulbaek Andersen *et al.*¹³ and was attributed to the presence of reactive impurities.

As stated in the Experimental section, in the present work an upper limit of 0.2% for the concentration of a potential impurity in the reactor is considered. The contribution of the OH-reaction with the potential impurity has been estimated considering two scenarios. When an OH-rate coefficient for the potential impurity is assumed to be on the order of $10^{-11}\text{ cm}^3\text{ molecule}^{-1}\text{ s}^{-1}$, as Sulbaek Andersen *et al.*¹³ assumed in their work, to obtain $k_1(298\text{ K})$ and $k_2(298\text{ K})$ consistent with the experimental ones, these rate coefficients would be more than one order of magnitude lower than those reported here and by other authors.^{13,19,20,22} So, the impurity, if any, is not reacting that fast with OH. When the OH-rate coefficient for the potential impurity is assumed to be below $10^{-12}\text{ cm}^3\text{ molecule}^{-1}\text{ s}^{-1}$, calculated $k_1(298\text{ K})$ and $k_2(298\text{ K})$ are within the experimental uncertainties and no effect would be noticeable on the measured $k_1(298\text{ K})$ and $k_2(298\text{ K})$. Therefore, we are confident in the results presented in Table 1.

The current JPL¹⁶ recommendation for $k_1(298\text{ K})$ is an average of the results from Langbein *et al.*,²⁰ Sulbaek Andersen

et al.,¹³ and Tokuhashi *et al.*¹² ($1.5 \times 10^{-14} \text{ cm}^3 \text{ molecule}^{-1} \text{ s}^{-1}$). The obtained k_1 (298 K) is somehow higher, as the recommended value is essentially that reported by Sulbaek Andersen *et al.*¹³ For sevoflurane, the JPL¹⁶ recommended value for k_2 (298 K) = $3.5 \times 10^{-14} \text{ cm}^3 \text{ molecule}^{-1} \text{ s}^{-1}$ is an average of the values from the relative rate and absolute measurements of Sulbaek Andersen *et al.*,¹³ with which this work is in agreement.

3.2. Infrared and ultraviolet absorption cross sections

3.2.1. Absolute and integrated IR absorption cross sections. In the ESI,† a text file lists the absolute $\sigma_{\tilde{\nu}}$ values for isoflurane and sevoflurane at 1 cm^{-1} intervals between 500 and 4000 cm^{-1} . The IR spectra obtained between 650 and 1650 cm^{-1} for the investigated HAGs are depicted as black lines in Fig. 3, while IR spectra previously reported in the literature are plotted as dashed lines. As Brown *et al.*¹⁸ did not list absolute $\sigma_{\tilde{\nu}}$ for isoflurane and sevoflurane, the IR spectra reported in Fig. 1 in ref. 18 have been digitalized and converted into $\sigma_{\tilde{\nu}}$ (in base *e*, as in this work) for comparison purposes. Above 2950 cm^{-1} , isoflurane and sevoflurane present negligible absorption and a very weak band in the 2950 – 3100 cm^{-1} range. Hence, this portion of the spectra is not shown in Fig. 3.

In Table S3,† the position and value of the maximum absorption cross section, $\sigma_{\tilde{\nu},\text{max}}$, are listed together with those

reported in the literature. The maximum absorption peak for isoflurane and sevoflurane is located at 1166.3 cm^{-1} and 1238.7 cm^{-1} , respectively, which is in agreement with those reported in the literature. In general, we observe a good agreement with the IR spectra reported by Sulbaek Andersen *et al.*¹⁰ in the entire wavenumber range. The largest difference was observed in $\sigma_{\tilde{\nu},\text{max}}$. Our reported values of $\sigma_{\tilde{\nu},\text{max}}$ are *ca.* 3% higher than those reported by Sulbaek Andersen *et al.*¹⁰ for isoflurane and *ca.* 5% higher for sevoflurane. However, this difference remains within the experimental uncertainties. With respect to $\sigma_{\tilde{\nu},\text{max}}$ reported by Brown *et al.*,¹⁸ there is a difference of *ca.* 20% when the value obtained in this work is compared. However, this difference in $\sigma_{\tilde{\nu}}$ values is observed in the entire wavenumber range. This discrepancy can be due to the lower instrumental resolution used by Brown *et al.*¹⁸ since the digitalization process of the IR spectra may account for less than 2% uncertainty in $\sigma_{\tilde{\nu}}$ values. This was confirmed by digitalizing our IR spectra from Fig. 3. No change in the position of the bands was observed either.

Table S4† summarizes $S_{\text{int}}(\tilde{\nu}_1 - \tilde{\nu}_2)$ over two wavenumber ranges to compare with previous studies. For isoflurane, $S_{\text{int}}(800$ – 1200 cm^{-1}) obtained here is higher than that reported by Brown *et al.*,¹⁸ while it is in agreement with that calculated by Sulbaek Andersen *et al.*,¹⁰ within our experimental uncertainties. Similarly, $S_{\text{int}}(650$ – 1500 cm^{-1}) from Sulbaek Andersen *et al.*¹⁰ is within the error limits of the present work, since these authors reported an uncertainty of 5%. For sevoflurane both $S_{\text{int}}(800$ – 1200 cm^{-1}) and $S_{\text{int}}(650$ – 1500 cm^{-1}) reported in the present study are in excellent agreement with those reported by Brown *et al.*¹⁸ and Sulbaek Andersen *et al.*¹⁰

3.2.2. UV absorption cross sections between 190 and 400 nm. UV absorption cross sections between 190 and 400 nm of isoflurane and sevoflurane are listed at 0.5 nm intervals in the text file provided in the ESI.† In Fig. 4, the UV spectra obtained are depicted together with those from the literature from 115 to 400 nm. In the inset of this figure a zoomed-in image of the UV spectra is presented from 180 to 230 nm for isoflurane and from 180 to 340 nm for sevoflurane. As shown for isoflurane, the spectrum obtained in this work agrees with that from Langbein *et al.*,²⁰ although their σ_{λ} are *ca.* 20% and 80% higher on average in the range of 200–210 nm and 215–230 nm, respectively. However, σ_{λ} from Lange *et al.*²³ is larger compared to that in Langbein *et al.*²⁰ and ours, especially above 205 nm. Lange *et al.*²³ observed a fine structure in this region (wavelength spacing, $\Delta\lambda = 0.5 \text{ nm}$), which is not observed in our work ($\Delta\lambda = 0.5 \text{ nm}$) and the work by Langbein *et al.*²⁰ ($\Delta\lambda = 0.1 \text{ nm}$). For sevoflurane, our results are in agreement with those of Langbein *et al.*,²⁰ who reported that this HAG does not show any absorption above 200 nm. Surprisingly, Lange *et al.*²³ observed structured absorption features above 200 nm with σ_{λ} up to $1.6 \times 10^{-20} \text{ cm}^2 \text{ molecule}^{-1}$. For hydrofluoroethers, no fine structure has been observed above 200–210 nm.²⁴ Moreover, σ_{λ} values of $10^{-20} \text{ cm}^2 \text{ molecule}^{-1}$ can be accurately measured in our system; however we did not observe any absorption, like Langbein *et al.*²⁰ These authors stated that the accuracy of their measured absorption cross sections was better than $\pm 5\%$. Considering our uncertainties in σ_{λ} above 200 nm due to the

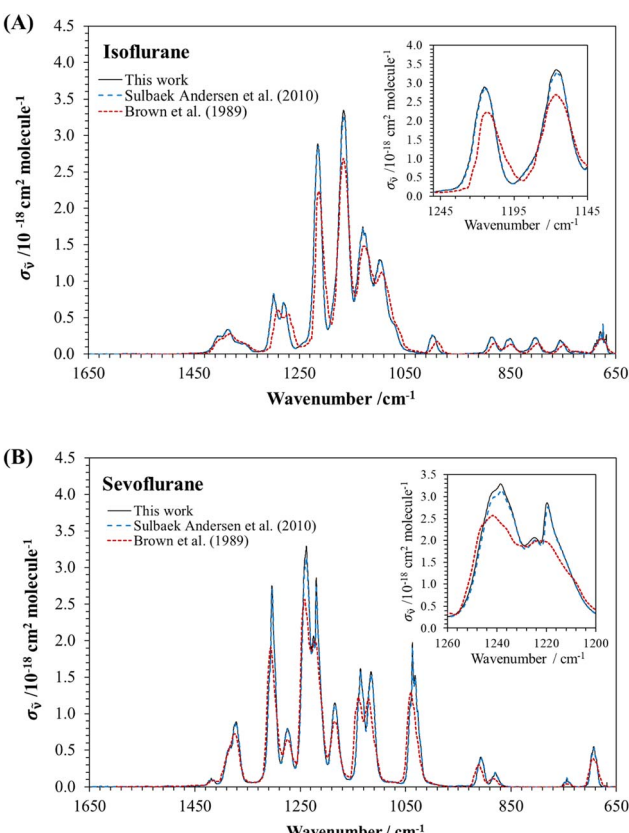


Fig. 3 Infrared absorption cross sections (in base *e*) between 650 and 1650 cm^{-1} for (A) isoflurane and (B) sevoflurane obtained in this work together with the literature spectra. The most intense band for each HAG is depicted in the insets.



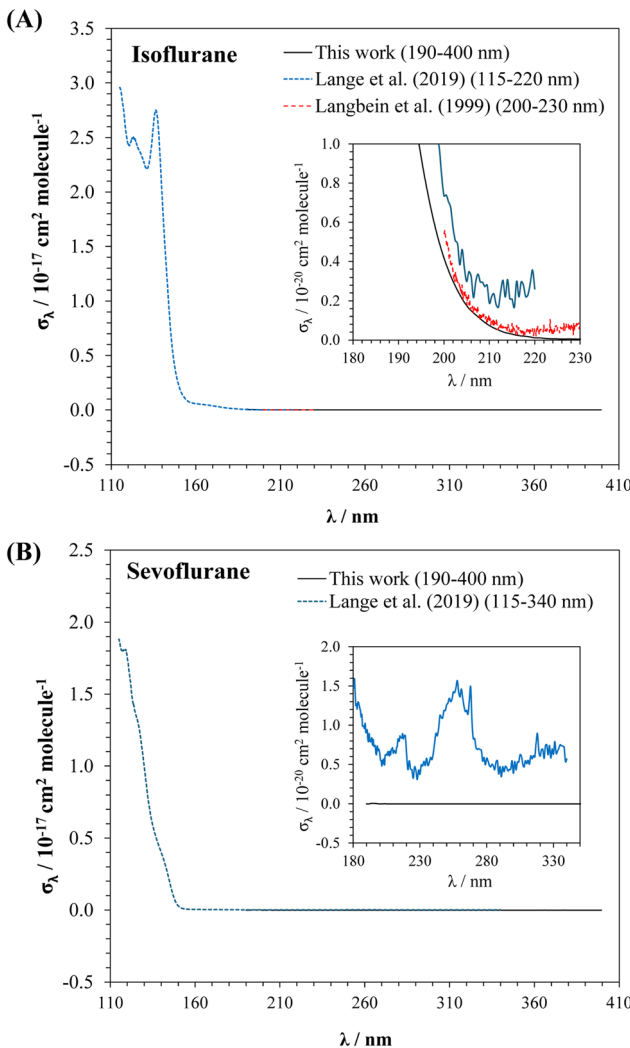


Fig. 4 UV absorption cross sections for isoflurane (A) and sevoflurane (B) between 115 and 400 nm.

very weak absorption of isoflurane, both studies are consistent (Fig. 4).

4. Atmospheric implications

4.1. Lifetime calculations

Chemical pathways such as the gas-phase reaction with atmospheric oxidants, like OH radicals and Cl atoms, and UV photolysis may govern the removal of isoflurane and sevoflurane in the atmosphere. The contribution of these processes to the global removal of these HAGs is given by the corresponding individual lifetime (τ).

For gases with lifetimes greater than few months, the atmospheric lifetime due to the reaction with OH is usually estimated relative to CH_3CCl_3 at the tropospheric mean temperature, 272 K.³⁰ For the investigated HAGs, $\tau_{\text{HAG}}^{\text{OH}}$ was calculated according to eqn (E10).

$$\tau_{\text{HAG}}^{\text{OH}} = \frac{k_{\text{OH}+\text{CH}_3\text{CCl}_3}(272 \text{ K})}{k_i(272 \text{ K})} \times \tau_{\text{CH}_3\text{CCl}_3}^{\text{OH}} \quad (\text{E10})$$

where $\tau_{\text{CH}_3\text{CCl}_3}^{\text{OH}}$ is the atmospheric lifetime of CH_3CCl_3 due to reaction with OH (5.99 years) and $k_{\text{OH}+\text{CH}_3\text{CCl}_3}(272 \text{ K})$ is $6.03 \times 10^{-15} \text{ cm}^3 \text{ molecule}^{-1} \text{ s}^{-1}$.^{31,32} The rate coefficients $k_1(272 \text{ K}) = (1.19 \pm 0.43) \times 10^{-14} \text{ cm}^3 \text{ molecule}^{-1} \text{ s}^{-1}$ and $k_2(272 \text{ K}) = (3.11 \pm 1.05) \times 10^{-14} \text{ cm}^3 \text{ molecule}^{-1} \text{ s}^{-1}$ were derived from eqn (E4) and (E5) determined in the present work. Therefore, the estimated $\tau_{\text{HAG}}^{\text{OH}}$ is 3.0 years and 1.2 years for isoflurane and sevoflurane, respectively. As shown in Table 3, current recommendations by WMO⁸ and IPCC⁷ (3.7 and 1.5 years, respectively) are higher than $\tau_{\text{HAG}}^{\text{OH}}$ estimated in this work and those from Sulbaek Andersen *et al.*¹³

Most of the values of $\tau_{\text{HAG}}^{\text{OH}}$ presented in Table 3 were estimated using $k_i(T)$ at the tropospheric average temperature (272–277 K) (see Table S5† for details). For both HAGs, Brown *et al.*¹⁹ estimated $\tau_{\text{HAG}}^{\text{OH}}$ relative to CH_3CCl_3 , while Sulbaek Andersen *et al.*¹³ used an average OH concentration of 10^6 radicals per cm^3 , in very good agreement with those obtained in our work. These $\tau_{\text{HAG}}^{\text{OH}}$ estimated from $k_i(272\text{--}277 \text{ K})$ varies from 2.0 to 3.2 years for isoflurane and from 0.9 to 1.2 years for sevoflurane. As shown in Table 2, Langbein *et al.*²⁰ reported much longer $\tau_{\text{HAG}}^{\text{OH}}$. This difference is not only attributable to a smaller rate coefficient. In fact, if $\tau_{\text{HAG}}^{\text{OH}}$ are estimated relative to CH_3CCl_3 , as was done in our work, and assuming their $k_i(298 \text{ K})$, the values are not as different as those reported in our work and in the bibliography ($\tau_{\text{HAG}}^{\text{OH}} = 2.12$ years for isoflurane; $\tau_{\text{HAG}}^{\text{OH}} = 1.33$ years for sevoflurane). Therefore, the main difference seems to be the use of the one-dimensional photochemical transport model. In this model, the concentration profile of OH with altitude between 0 and 36 km was considered and a constant value of $k_i(298 \text{ K})$ was assumed through the troposphere and stratosphere.

The lifetime of isoflurane and sevoflurane due to Cl-reaction ($\tau_{\text{HAG}}^{\text{Cl}}$) can be estimated from eqn (11), using a 24-h average Cl concentration, $[\text{Cl}]_{24\text{h}}$, of 10^3 cm^{-3} (ref. 33) and the rate coefficient for the Cl-reaction at room temperature: $(4.5 \pm 0.8) \times 10^{-15} \text{ cm}^3 \text{ molecule}^{-1} \text{ s}^{-1}$ for isoflurane and $(1.1 \pm 0.1) \times 10^{-13} \text{ cm}^3 \text{ molecule}^{-1} \text{ s}^{-1}$ for sevoflurane.¹³

$$\tau_{\text{HAG}}^{\text{Cl}} = \frac{1}{k_{\text{Cl}}[\text{Cl}]_{24\text{h}}} \quad (\text{E11})$$

Estimates of $\tau_{\text{HAG}}^{\text{Cl}}$ for isoflurane and sevoflurane are extremely long (>7000 years and around 290 years, respectively) compared to $\tau_{\text{HAG}}^{\text{OH}}$. Clearly, the chemical lifetime of isoflurane and sevoflurane is governed by their reaction with OH radicals.

As shown in Fig. S8,† σ_{λ} for isoflurane is very low in the UV solar actinic region ($\lambda > 290 \text{ nm}$) and presents large uncertainties (grey lines) due to this very weak absorption. Sevoflurane presents even lower absorption. Considering the long lifetime of these HAGs, they are likely to be transported to the stratosphere. Overlapping the spectral actinic flux (F_{λ}) at two altitudes (0 km – troposphere- and 36 km – stratosphere) with the UV spectra of these HAGs, it is expected that photolysis is not an important removal process in the atmosphere, as concluded by Langbein *et al.*²⁰ These authors averaged the photolysis rate (β) of isoflurane over 24 h and integrated it between 0 and 36 km altitude (z) at a geographical latitude of 50°N in the equinox. To confirm this, the upper limit of J

Table 3 Atmospheric lifetimes, radiative efficiencies (REs), and GWPs at a time horizon of 100 years relative to CO₂. Recalculated values are indicated in bold

| Anesthetic | $\tau_{\text{HAG}}^{\text{OH}}/\text{years}$ | RE _i /W m ⁻² ppbv ⁻¹ | Lifetime-corrected RE _i /W m ⁻² ppbv ⁻¹ | GWP _{100 years} | Reference |
|-------------|--|---|--|--------------------------|--|
| Isoflurane | 3.0 | 0.50 | 0.44 | 508 | This work |
| | 3.7 | n. r. | 0.43 ^a | 539 | IPCC ⁷ |
| | 3.7 | n. r. | 0.43 ^a | 536 | WMO ⁸ |
| | 3.7 | 0.47 ^b | 0.43 | 565 | Hodnebrog <i>et al.</i> ¹⁷ |
| | 3.2 | 0.45 ^c | 0.40 | 489 | Sulbaek Andersen <i>et al.</i> ¹³ |
| | 5.1 | n. r. | — | 625 | Langbein <i>et al.</i> ²⁰ |
| | 2.0 | n. r. | — | 311 | Brown <i>et al.</i> ¹⁹ |
| Sevoflurane | 1.2 | 0.39 | 0.30 | 125 | This work |
| | 1.5 | n. r. | 0.31 ^a | 195 | IPCC ⁷ |
| | 1.5 | n. r. | 0.31 ^a | 140 | WMO ⁸ |
| | 1.4 | | | 127/144 ^d | Sulbaek Andersen <i>et al.</i> ¹⁵ |
| | 1.9 | 0.37 ^b | 0.31 | 205 | Hodnebrog <i>et al.</i> ¹⁷ |
| | 1.1 | 0.35 ^c | 0.27 | 102 | Sulbaek Andersen <i>et al.</i> ¹³ |
| | 4.0 | n. r. | — | 250 | Langbein <i>et al.</i> ²⁰ |
| | 0.9 | n. r. | — | 62 | Brown <i>et al.</i> ¹⁹ |

^a Taken from Hodnebrog *et al.*¹⁷ ^b Taken from Hodnebrog *et al.*³⁷ ^c Taken from Sulbaek Andersen *et al.*¹⁰ ^d See text.

between 0 and 36 km was also estimated here from F_{λ} taken from the NCAR ACOM TUV model³⁴ for a summer solstice day in a medium latitude city in Spain (39°N). Assuming a photolysis quantum yield of 1 for isoflurane, as Langbein *et al.*²⁰ did, and considering the uncertainties in σ_{λ} , an upper limit of J would be $(1.42 \pm 10.1) \times 10^{-7} \text{ s}^{-1}$ which yields a lower limit for the lifetime due to photolysis ($\tau_{\text{HAG}}^{\text{Photo}}$) of (81 ± 578) days. Langbein *et al.*²⁰ considered σ_{λ} between 200 and 230 nm in their calculations reporting a $\tau_{\text{HAG}}^{\text{Photo}}$ of 3130 years for isoflurane. Given the extremely high uncertainties in J and $\tau_{\text{HAG}}^{\text{Photo}}$, it cannot be conclusively stated that UV photolysis of isoflurane in the troposphere and stratosphere constitutes a significant removal pathway. For sevoflurane, since σ_{λ} determined in this work is negligible, within the extremely large uncertainties in the evaluated λ range, it is inappropriate to estimate $\tau_{\text{HAG}}^{\text{Photo}}$. Langbein *et al.*²⁰ did not report $\tau_{\text{HAG}}^{\text{Photo}}$ of sevoflurane due to its negligible UV absorption.

4.2. Radiative efficiencies and GWPs

REs (in W m⁻² ppbv⁻¹) and GWP_{100 years} of HAGs were calculated using the same methodology as in our previous studies.²⁶ The instantaneous RE (in W m⁻² ppbv⁻¹) for isoflurane and sevoflurane was calculated for a 0–1 ppbv increase in mixing ratio from the integrated IR absorption cross sections in 1 cm⁻¹ between 500 and 3000 cm⁻¹ and using the radiative forcing per integrated absorption cross section parameterized in 1-cm⁻¹ intervals, F' (in W m⁻² (cm⁻¹)⁻¹ (cm² molecule⁻¹)⁻¹), from Hodnebrog *et al.*¹⁷

$$\text{RE}_i \cong \sum_{500 \text{ cm}^{-1}}^{3000 \text{ cm}^{-1}} S_{\text{int}} F' \quad (\text{E12})$$

The obtained instantaneous REs for isoflurane were 0.50 W m⁻² ppbv⁻¹ and 0.39 W m⁻² ppbv⁻¹ for sevoflurane. These values were corrected with the fractional correction factor (f_{τ}) defined in eqn (E13).³⁵

$$f_{\tau} = \frac{2.962(\tau_{\text{HAG}}^{\text{OH}})^{0.9312}}{1 + 2.994(\tau_{\text{HAG}}^{\text{OH}})^{0.9302}} \quad (\text{E13})$$

The obtained f_{τ} was 0.885 and 0.767 for isoflurane and sevoflurane, respectively. The lifetime-corrected RE was then obtained by multiplying RE_i with f_{τ} . These parameters were 0.44 and 0.30 W m⁻² ppbv⁻¹ for isoflurane and sevoflurane, respectively, which are in excellent agreement with current recommendations by the WMO⁸ and IPCC⁷, which are based on the lifetime-corrected REs from Hodnebrog *et al.*¹⁷ (see Table 3). REs from the literature have been recalculated for comparison purposes, considering the corresponding f_{τ} and $\tau_{\text{HAG}}^{\text{OH}}$ and are listed in Table 3. The lifetime-corrected REs from the instantaneous RE_i calculated in this study are 10% higher than the ones reported by Sulbaek Andersen *et al.*¹³ (0.40 W m⁻² ppb⁻¹ for isoflurane and 0.27 W m⁻² ppb⁻¹ for sevoflurane), mainly due to the observed difference in the maximum absorption cross section of the HAGs, since f_{τ} factors in Sulbaek Andersen *et al.*¹³ and in this work are very similar.

In this work, the lifetime-corrected REs were used to calculate GWP_{100 years} of HAGs using eqn (E14).

$$\text{GWP}_{100 \text{ years}} = f_{\tau} \frac{\text{RE}_i \tau_{\text{HAG}}^{\text{OH}} (1 - \exp(-100 \text{ years} / \tau_{\text{HAG}}^{\text{OH}}))}{\text{AGWP}(\text{CO}_2)} \quad (\text{E14})$$

where RE_i is the instantaneous radiative efficiency due to a unit increase in atmospheric abundance of the gas (in W m⁻² kg⁻¹) and AGWP(CO₂)¹⁷ is the absolute GWP of CO₂ for the same time horizon, $8.06 \times 10^{-14} \text{ W m}^{-2} \text{ yr} (\text{kg CO}_2)^{-1}$. As shown in Table 3, GWP_{100 years} = 508 for isoflurane and GWP_{100 years} = 125 for sevoflurane.

The values reported by Langbein *et al.*²⁰ were relative to CFC-12 (CF₂Cl₂) and those reported by Brown *et al.*¹⁹ were relative to CFC-11 (CFCl₃). Therefore, we expressed these GWP_{100 years} relative to CO₂ by using GWP_{100 years} for CFC-11 and CFC-12 taken from the IPCC⁷ (6230 and 12 500, respectively). All GWP_{100 years} listed in Table 3 are then relative to CO₂. Although

Brown *et al.*¹⁹ reported the infrared integrated absorption cross sections for isoflurane and sevoflurane between 800 and 1200 cm⁻¹, and used them to calculate GWP_{100 years} (311 for isoflurane and 62 for sevoflurane), no RE values were reported and GWP_{100 years} is not lifetime-corrected. Moreover, our GWP_{100 years} for isoflurane and sevoflurane are 63% and 102% higher than that of Brown *et al.*¹⁹ and are much lower than those in the rest of studies due to smaller atmospheric lifetimes (see Table 3). Similarly, Langbein *et al.*²⁰ calculated GWP_{100 years} using the IR integrated absorption cross section provided by Brown *et al.*¹⁸ and showed larger lifetimes than Brown *et al.*¹⁹ As a consequence, GWP_{100 years} was higher than previously reported by Brown and coworkers (625 for isoflurane and 250 for sevoflurane). If our results are compared with theirs, the reported GWP_{100 years} for isoflurane is 19% lower, while it is half for sevoflurane. This large difference is due to the non-correction of REs with the HAG lifetime. If this lifetime correction is applied to REs reported by Sulbaek Andersen *et al.*,¹³ our GWP_{100 years} is 4% lower than theirs for isoflurane (GWP_{100 years} = 489) and 22% higher for sevoflurane (GWP_{100 years} = 102). For sevoflurane, Sulbaek Andersen *et al.*¹⁵ updated GWP_{100 years} calculations considering an atmospheric lifetime of 1.4 years based on the JPL recommendation.¹⁶ They determined a GWP_{100 years} of 127 when using AGWP(CO₂) from IPCC 2013³⁶ and 144 when using the updated AGWP(CO₂) from Hodnebrog *et al.*¹⁷ GWP_{100 years} recommended in this work agrees with their first updated calculation and is 13% lower than the last one.

GWP_{100 years} for sevoflurane reported here and from the study of Sulbaek Andersen *et al.*¹⁵ is notably lower than current recommendations of GWP_{100 years} by the WMO³¹ and IPCC.² Sulbaek Andersen *et al.*¹⁵ provided further evidence that these recommendations need to be modified.

5. Conclusions

A comprehensive study on temperature dependence of the absolute OH-rate coefficients for isoflurane and sevoflurane has been carried out in this work at temperatures above and below 298 K. Our results confirm the observed *T*-dependencies of *k*₁(*T*) and *k*₂(*T*) recommended by JPL,¹⁶ expanding the *T* range of the Sulbaek Andersen *et al.*¹³ study on which the recommendation is based. Both reactions present positive low activation energies of around 9 kJ mol⁻¹. The knowledge of the OH-rate coefficients at the average atmospheric temperature (272 K) is essential to accurately calculate the atmospheric chemical lifetime of these inhaled anesthetics. In this work, we report *k*₁(272 K) = 1.31 × 10⁻¹⁴ cm³ molecule⁻¹ s⁻¹ and *k*₂(272 K) = 3.04 × 10⁻¹⁴ cm³ molecule⁻¹ s⁻¹ and used them to derive $\tau_{\text{HAG}}^{\text{OH}}$, 3.0 years for isoflurane and 1.2 years for sevoflurane. These $\tau_{\text{HAG}}^{\text{OH}}$ are lower than those currently recommended by the WMO⁸ and IPCC.⁷ This directly impacts the resulting lifetime-corrected radiative efficiencies and, therefore, global warming potentials, GWP_{100 years} = 457 and 125 respectively. The obtained values of GWP_{100 years} are also lower than current recommendations. As the calculated lifetime-corrected radiative efficiencies for isoflurane and sevoflurane are in excellent accordance with previous

studies, the decrease in $\tau_{\text{HAG}}^{\text{OH}}$ led to differences in GWP_{100 years} with respect to the recommended ones by the WMO⁸ and IPCC.⁷ For isoflurane, this difference is 5%; however, for sevoflurane, the difference in GWP_{100 years} is 11% with respect to the recommended value by the WMO⁸ and 36% with respect to the IPCC.⁷

In summary, this work updates the current recommendations of $\tau_{\text{HAG}}^{\text{OH}}$ and GWP_{100 years} for isoflurane and sevoflurane, confirming that, according to the EU 2024 regulation,⁶ isoflurane is a high-GWP gas (GWP_{100 years} > 150), while sevoflurane does not meet the high-GWP threshold. A reassessment of the IPCC and WMO values is recommended.

Data availability

The data supporting this article have been included as part of the ESI.†

Author contributions

S. Espinosa: experiments, formal analysis, writing the original draft, review and editing. F. Martínez: experiments, formal analysis, writing the original draft, writing, review and editing. M. Antiñolo: methodology, formal analysis, review and editing. Ole J. Nielsen: conceptualization, methodology, formal analysis. E. Jiménez: conceptualization, supervision, funding acquisition, formal analysis, review and editing.

Conflicts of interest

There are no conflicts to declare.

Acknowledgements

This work has been supported by the INTERESFERA project (Ref. SBPLY/23/180225/000054) funded by the regional government of Castilla-La Mancha (JCCM), the European Regional Development Fund (FEDER) and by the HALOGAS project (Ref. PID2023-146369OB-I00) awarded by the Spanish Ministry of Science, Innovation and Universities (MICIU). This research has also been partially supported by the University of Castilla-La Mancha – UCLM through the Ayudas para la financiación de actividades de investigación dirigidas a grupos (Ref. 2022-GRIN-34143). S. Espinosa also acknowledges the CHEMLIFE project (Ref. PID2020-113936GB-I00 awarded by the Spanish MCIN/AEI) for funding her contract during the performance of this investigation. F. Martínez acknowledges the INVESTIGO program of UCLM funded by JCCM through the European Social Funds Plan of Castilla-La Mancha 2021–2027. We thank Prof. Pilar Martín for helping in the GC/MS analysis of the HAG samples.

References

- 1 M. K. Vollmer, T. S. Rhee, M. Rigby, D. Hofstetter, M. Hill, F. Schoenenberger and S. Reimann, Abrupt reversal in emissions and atmospheric abundance of HCFC-133a (CF₃CH₂Cl), *Geophys. Res. Lett.*, 2015, **42**, 1606–1611.



2 Y. Ishizawa, General anesthetic gases and the global environment, *Anesth. Analg.*, 2011, **112**, 213–217.

3 Ministry of Health, *Annual Report of the National Health System 2022 Reports, Studies and Research*, 2023.

4 O. J. Nielsen and M. P. Sulbaek Andersen, Inhalational volatile anaesthetic agents: the atmospheric scientists' viewpoint, *Anaesthesia*, 2024, **79**, 246–251.

5 I. Tennison, S. Roschnik, B. Ashby, R. Boyd, I. Hamilton, T. Oreszczyn, A. Owen, M. Romanello, P. Ruysssevelt, J. D. Sherman, A. Z. P. Smith, K. Steele, N. Watts and M. J. Eckelman, Health care's response to climate change: a carbon footprint assessment of the NHS in England, *Lancet Planet. Health*, 2021, **5**, 84–92.

6 Regulation 2024/573, Regulation (EU) 2024/573 of the European Parliament and of the Council of 7 February 2024 on fluorinated greenhouse gases, amending Directive (EU) 2019/1937 and repealing Regulation (EU) No 517/2014 Regulation (EU) No 1143/2014 of the European Parliament and of the Council of 22 October 2014 on the prevention and management of the introduction and spread of invasive alien species, <http://data.europa.eu/eli/reg/2024/573/oj>.

7 Intergovernmental Panel on Climate Change (IPCC), Climate Change Summary for Policymakers, in *Climate Change 2023: Synthesis Report. Contribution of Working Groups I, II and III to the Sixth Assessment Report of the Intergovernmental Panel on Climate Change*, ed. Core Writing Team, H. Lee and J. Romero, IPCC, Geneva, Switzerland, pp. , pp. 1–34.

8 World Meteorological Organization (WMO), *Scientific Assessment of Ozone Depletion: 2022: Executive Summary*, 2022, p. 56, G. R. No. 278, W. G. S.

9 H. Gadani and A. Vyas, Anesthetic gases and global warming: Potentials, prevention and future of anesthesia, *Anesth. Essays Res.*, 2011, **5**, 5–10.

10 M. P. Sulbaek Andersen, S. P. Sander, O. J. Nielsen, D. S. Wagner, T. J. Sanford and T. J. Wallington, Inhalation anaesthetics and climate change, *Br. J. Anaesth.*, 2010, **105**, 760–766.

11 W. B. DeMore, Regularities in Arrhenius parameters for rate constants of abstraction reactions of hydroxyl radical with C–H bonds, *J. Photochem. Photobiol. A*, 2005, **176**, 129–135.

12 K. Tokuhashi, A. Takahashi, M. Kaise and S. Kondo, Rate constants for the reactions of OH radicals with $\text{CH}_3\text{OCF}_2\text{CHFCl}$, $\text{CHF}_2\text{OCF}_2\text{CHFCl}$, $\text{CHF}_2\text{OCHClCF}_3$, and $\text{CH}_3\text{CH}_2\text{OCF}_2\text{CHF}_2$, *J. Geophys. Res. Atmos.*, 1999, **104**, 18681–18688.

13 M. P. Sulbaek Andersen, O. J. Nielsen, B. Karpichev, T. J. Wallington and S. P. Sander, Atmospheric chemistry of isoflurane, desflurane, and sevoflurane: kinetics and mechanisms of reactions with chlorine atoms and OH radicals and global warming potentials, *J. Phys. Chem. A*, 2012, **116**, 5806–5820.

14 M. P. Sulbaek Andersen, O. J. Nielsen and J. D. Sherman, Assessing the potential climate impact of anaesthetic gases, *Lancet Planet. Health*, 2023, **7**, e622–e629.

15 M. P. Sulbaek Andersen, O. J. Nielsen and J. D. Sherman, The Global Warming Potentials for Anesthetic Gas Sevoflurane Need Significant Corrections, *Environ. Sci. Technol.*, 2021, **55**, 10189–10191.

16 J. B. Burkholder, S. P. Sander, J. Abbatt, J. R. Barker, C. Cappa, J. D. Crounse, T. S. Dibble, R. E. Huie, C. E. Kolb, M. J. Kurylo, V. L. Orkin, C. J. Percival, D. M. Wilmouth, and P. H. Wine, *Chemical Kinetics and Photochemical Data for Use in Atmospheric Studies, Evaluation No. 19*, JPL Publication 19-5, Jet Propulsion Laboratory, Pasadena, 2019, <http://jpldataeval.jpl.nasa.gov>.

17 Ø. Hodnebrog, B. Aamaas, J. S. Fuglestvedt, G. Marston, G. Myhre, C. J. Nielsen, M. Sandstad, K. P. Shine and T. J. Wallington, Updated Global Warming Potentials and Radiative Efficiencies of Halocarbons and Other Weak Atmospheric Absorbers, *Rev. Geophys.*, 2020, **58**, e2019RG000691.

18 A. C. Brown, C. E. Canosa-Mas, A. D. Parr, J. M. T. Pierce and R. P. Wayne, Tropospheric lifetimes of halogenated anaesthetics, *Nature*, 1989, **341**, 635–637.

19 A. C. Brown, C. E. Canosa-Mas, A. D. Parr and R. P. Wayne, Laboratory studies of some halogenated ethanes and ethers: Measurements of rates of reaction with OH and of infrared absorption cross-sections, *Atmos. Environ.*, 1990, **24**, 2499–2511.

20 T. Langbein, H. Sonntag, D. Trapp, A. Hoffmann, W. Malms, E.-P. Röth, V. Mörs and R. Zellner, Volatile anaesthetics and the atmosphere, *Br. J. Anaesth.*, 1999, **82**, 66–73.

21 S. Nolan, N. O'Sullivan, J. Wenger, H. Sidebottom and J. Treacy, Kinetics and Mechanisms of the OH Radical Initiated Degradation of a Series of Hydrofluoroethers, *Trans. Ecol. Environ.*, 1999, **28**, 120–123.

22 S. D. Beach, K. M. Hickson, I. W. M. Smith and R. P. Tuckett, Rate constants and Arrhenius parameters for the reactions of OH radicals and Cl atoms with $\text{CF}_3\text{CH}_2\text{OCHF}_2$, $\text{CF}_3\text{CHClOCHF}_2$ and $\text{CF}_3\text{CH}_2\text{OCClF}_2$, using the discharge-flow/resonance fluorescence method, *Phys. Chem. Chem. Phys.*, 2001, **3**, 3064–3069.

23 E. Lange, F. Ferreira Da Silva, N. C. Jones, S. V Hoffmann, D. Duflot and P. Limão-Vieira, The lowest-lying electronic states of isoflurane and sevoflurane in the 5.0–10.8 eV energy range investigated by experimental and theoretical methods, *Chem. Phys. Lett.*, 2019, **716**, 42–48.

24 H. Keller-Rudek, G. K. Moortgat, R. Sander, and R. Sorensen, The MPI-Mainz UV/VIS Spectral Atlas of Gaseous Molecules of Atmospheric Interest, <https://essd.copernicus.org/articles/5/365/2013/>.

25 J. Albaladejo, B. Ballesteros, E. Jiménez, P. Martín and E. Martínez, A PLP-LIF Kinetic Study of the Atmospheric Reactivity of a Series of C4–C7 Saturated and Unsaturated Aliphatic Aldehydes with OH, *Atmos. Environ.*, 2002, **36**, 3231–3239.

26 (a) S. Blázquez, S. Espinosa, M. Antíñolo, J. Albaladejo and E. Jiménez, Kinetics of $\text{CF}_3\text{CH}_2\text{OCH}_3$ (HFE-263fb2), $\text{CHF}_2\text{CF}_2\text{CH}_2\text{OCH}_3$ (HFE-374pcf), and $\text{CF}_3\text{CF}_2\text{CH}_2\text{OCH}_3$ (HFE-365mcf3) with OH radicals, IR absorption cross sections, and global warming potentials, *Phys. Chem. Chem. Phys.*, 2022, **24**, 14354–14364; (b) S. Espinosa, M. Asensio, M. Antíñolo, J. Albaladejo and E. Jiménez,



Atmospheric chemistry of $\text{CF}_3\text{CHFCF}_2\text{OCH}_3$ (HFE-356mec3) and $\text{CHF}_2\text{CHFOCF}_3$ (HFE-236ea1) initiated by OH and Cl and their contribution to global warming, *Environ. Sci. Pollut. Res.*, 2024, **31**, 50347–50358.

27 E. Jiménez, B. Lanza, A. Garzón, B. Ballesteros and J. Albaladejo, Atmospheric Degradation of 2-Butanol, 2-Methyl-2-butanol, and 2,3-Dimethyl-2-butanol: OH Kinetics and UV Absorption Cross Sections, *J. Phys. Chem. A*, 2005, **109**, 10903–10909.

28 M. Antíñolo, E. Jiménez, A. Notario, E. Martínez and J. Albaladejo, Evaluation of the daytime tropospheric loss of 2-methylbutanal, *Atmos. Chem. Phys.*, 2010, **10**, 1911–1922.

29 S. Blázquez, D. González, E. M. Neeman, B. Ballesteros, M. Agúndez, A. Canosa, J. Albaladejo, J. Cernicharo and E. Jiménez, Gas-phase kinetics of CH_3CHO with OH radicals between 11.7 and 177.5 K, *Phys. Chem. Chem. Phys.*, 2020, **22**, 20562–20572.

30 C. M. Spivakovsky, J. A. Logan, S. A. Montzka, Y. J. Balkanski, M. Foreman-Fowler, D. B. A. Jones, L. W. Horowitz, A. C. Fusco, C. A. M. Brenninkmeijer, M. J. Prather, S. C. Wofsy and M. B. McElroy, Three-dimensional climatological distribution of tropospheric OH: Update and evaluation, *J. Geophys. Res. Atmos.*, 2000, **105**, 8931–8980.

31 M. J. Kurylo and V. L. Orkin, Determination of Atmospheric Lifetimes via the Measurement of OH Radical Kinetics, *Chem. Rev.*, 2003, **102**, 5049–5076.

32 R. G. Prinn, J. Huang, R. F. Weiss, D. M. Cunnold, P. J. Fraser, P. G. Simmonds, A. McCulloch, C. Harth, P. Salameh, S. O'Doherty, R. H. J. Wang, L. Porter and B. R. Miller, Evidence for substantial variations of atmospheric hydroxyl radicals in the past two decades, *Science*, 2001, **292**, 1882–1888.

33 H. B. Singh, A. N. Thakur, Y. E. Chen and M. Kanakidou, Tetrachloroethylene as an Indicator of low Cl Atom Concentrations in the Troposphere, *Geophys. Res. Lett.*, 1996, **23**, 1529–1532.

34 S. Madronich and S. Flocke, The Role of Solar Radiation in Atmospheric Chemistry, in *Environmental Photochemistry*, 1999, pp. 1–26.

35 K. P. Shine, G. Myhre, K. P. Shine and G. Myhre, The spectral nature of stratospheric temperature adjustment and its application to halocarbon radiative forcing, *J. Adv. Model. Earth Syst.*, 2020, **2020**(12), e2019MS001951.

36 T. F. Stocker, G.-K. D. Qin, M. Plattner, S. K. Tignor, J. Allen, A. Boschung, et al., *Climate Change 2013: the Physical Science Basis. Contribution of Working Group I to the Fifth Assessment Report of the Intergovernmental*, Cambridge University Press, IPCC, 2013, Cambridge, United Kingdom and New York, NY.

37 Ø. Hodnebrog, M. Etminan, J. S. Fuglestvedt, G. Marston, G. Myhre, C. J. Nielsen, K. P. Shine and T. J. Wallington, Global warming potentials and radiative efficiencies of halocarbons and related compounds: A comprehensive review, *Rev. Geophys.*, 2013, **51**, 300–378.

